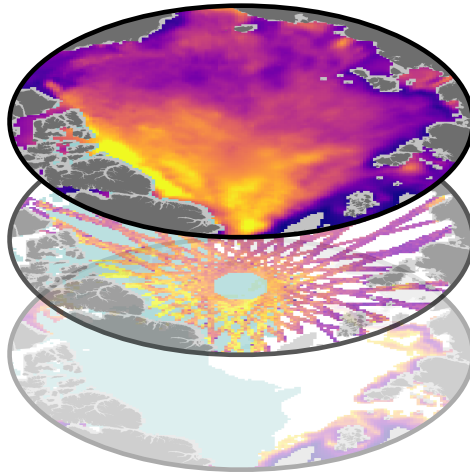


CS2SMOS

User Guide v3.0



Authors

Robert Ricker¹

Stefan Hendricks¹

Lars Kaleschke³

Xiangshan Tian-Kunze³

¹Alfred Wegener Institute, Helmholtz Centre for Polar and Marine Research, Bremerhaven

²University of Hamburg, Germany

Alfred-Wegener-Institut Helmholtz-Zentrum für Polar- und Meeresforschung

August 2016



Change Log

Document Rev.	Product Rev.	Date	Changes
1.0	1.0	02.12.2015	Initial version
2.0	1.1	01.06.2016	Major algorithm changes: New background field estimate New background field estimate New correlation length scale estimate Applying OSI SAF ice type product to exclude SMOS data over multiyear ice Documentation changes
2.1	1.1	23.08.2016	Minor changes in the document
2.1	1.2	23.11.2016	Minor changes: Added CS2/SMOS weighted mean field in netcdf files Added attributes in netcdf files Switch to netcdf version 4
3.0	1.3	05.06.2017	Major algorithm changes: This algorithm version refers to Ricker et al. (2017) SMOS background now uses one week behind and one week ahead of the target week Switching from SMOS product version 3.0 to 3.1 Documentation changes

Known Issues

Issue	Product Rev.	Status
Underestimation of SMOS ice thickness when ice concentration is low	1.3	Open
Fundamental calibration of CryoSat-2 range retracking algorithm required	1.3	Open
New data mask in OSI-401 v3.0 introduced in summer 2016 leads to inconsistency to former CS2SMOS retrievals	1.3	Corrected by using OSI-401 v2.2 data mask for the OSI-401 v3.0 product, requires further investigation

Important Note

This service is not an operational data service. Updates on weekly ice thickness fields will happen irregularly and revisions of the entire data time series might occur at any time. This product shall be a tool for the scientific community to enable further development of sea ice thickness retrieval algorithms and not be used in the sense of a fully calibrated and validated data product. It is our aim however, to implement progress in algorithm development in new revisions. We encourage users to give feedback (info@meereisportal.de) for further improvements of the CryoSat-2/SMOS merged product.

1 Introduction

1.1 Purpose of this document

The purpose of this document is to briefly describe the data merging and specifically the optimal interpolation algorithm of the CS2SMOS intermediate climate data record (ICDR), which has been developed within the framework of the SMOS+Sea ice project, funded by the European Space Agency. This document provides a description of the algorithm applied to merge the individual CryoSat-2 (CS2) and Soil Moisture and Ocean Salinity (SMOS) sea-ice thickness products, as well as output data format specifications. Furthermore, characteristics of the merged product are illustrated in order to inform about the differences to the individual products.

1.2 Motivation and Scope of the CS2-SMOS Data Merging

The SMOS mission provides L-band observations and the ice thickness-dependency of brightness temperature enables to estimate the sea-ice thickness for thin ice regimes, in particular during the freeze-up (Kaleschke et al., 2012). On the other hand, CS2 uses radar altimetry to measure the height of the ice surface above the water level, which can be converted into sea-ice thickness assuming hydrostatic equilibrium. In contrast to SMOS, The CS2 mission was primarily designed to measure the thickness of the perennial and thick first-year ice cover and lacks the sensitivity for thin ice regimes (Wingham et al., 2006).

The complementary nature of the relative uncertainties of CS2 and SMOS ice thickness retrievals has been shown by Kaleschke et al. (2015). Figure 1 illustrates uncertainty maps and the relative uncertainties of CS2 and SMOS monthly means from March 2016. While the SMOS relative uncertainties are lowest for very thin ice, CS2 relative thickness uncertainties are smaller over thick ice and rise asymptotic towards thickness values < 1 m, which is due to the different methodical approach. We acknowledge that the CS2 uncertainties represent random uncertainties only. Systematic errors as due to the usage of a snow climatology as well as snow-volume scattering may alter the uncertainty estimate (Ricker et al., 2014, 2015).

However, also the spatial coverage is of complementary nature due to the different orbital inclinations. Figure 2 shows weekly means of CS2 and SMOS during the freezing season

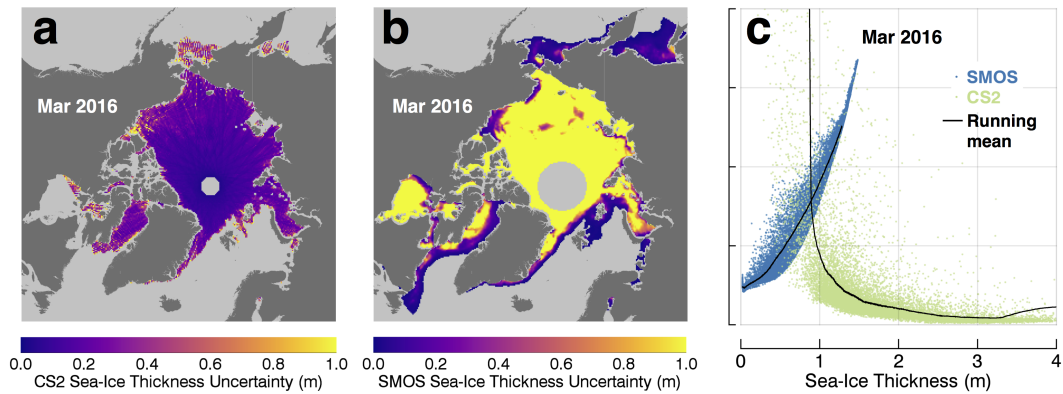


Figure 1: Monthly sea-ice thickness uncertainty maps of the CryoSat-2 (a) and SMOS (b) retrieval for March 2016. c) Relative uncertainties from March 2016.

2015/16. While valid SMOS ice thickness estimates can be found mostly in the marginal ice zones, the CS2 ice thickness retrieval covers major parts of the Arctic multiyear ice (MYI). Figure 3 illustrates the number of valid grid cells of the weekly means as shown in Figure 2. The number of grid cells, which share SMOS and CS2 estimates, is significantly lower than of grid cells that contain thickness estimates from one sensor exclusively.

Hence, merging of CS2 and SMOS sea-ice thickness retrievals has the capability to complete Arctic sea-ice thickness distributions. Therefore, we developed a method to merge both data sets on a suitable spatial and temporal scale.

1.3 Further Information

Additional information of the CryoSat-2 and SMOS missions as well as other ESA data products can be found on the following websites:

- [ESA - Living Planet Program- CryoSat-2](#)
- [ESA - Living Planet Program- SMOS](#)

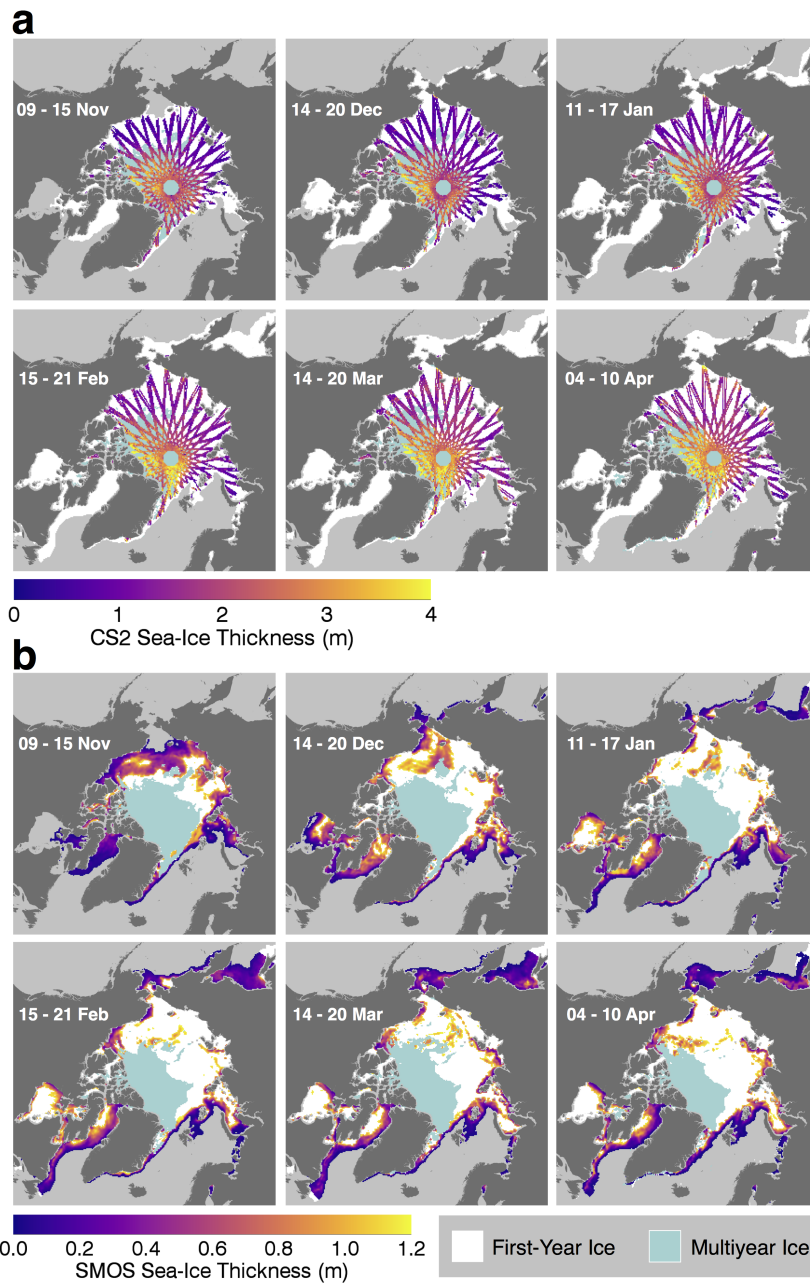


Figure 2: Weekly input data grids for the freezing season November-April 2015/16. a) Weekly CryoSat-2 retrieval as used for the optimal interpolation. b) Weekly means of daily SMOS ice thickness retrievals, cropped by a 1 m maximum SMOS thickness uncertainty filter. The background indicates first-year and multiyear ice coverage. Note the complementary coverage in a) and b).

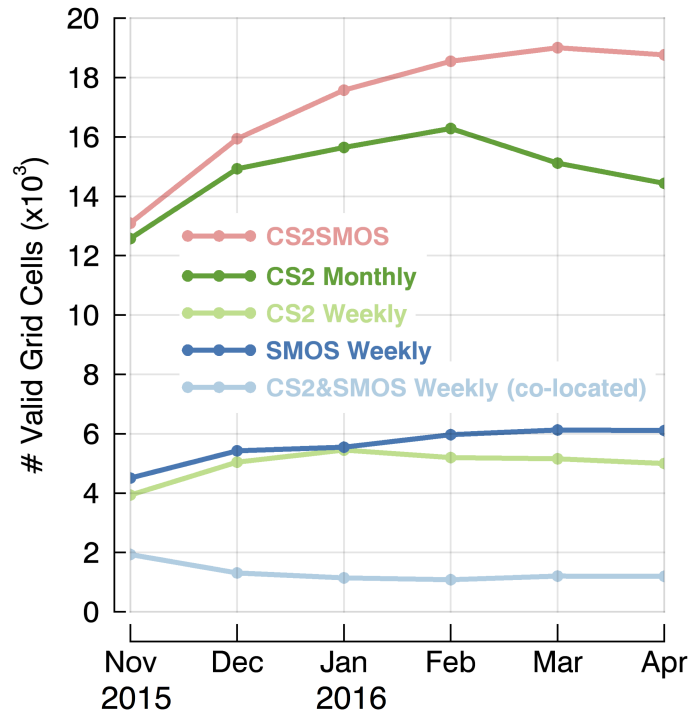


Figure 3: Spatial coverage in number of valid 25 km grid cells. Here, the term *valid* means that the grid cell contains a valid thickness estimate. The merged product and other gridded products are represented by weeks illustrated in Figure 2.

2 Methods

We use an optimal interpolation scheme (OI) similar to Böhme and Send (2005); Boehme et al. (2008); McIntosh (1990) that enables the merging of datasets from diverse sources on a predefined, so-called analysis grid. The data are weighted differently based on known uncertainties of the individual products and modeled spatial covariances. OI minimizes the total error of observations and provides ideal weighting for the observations at each grid cell.

In this section we present the processing methods, on which the here presented optimal interpolation is based on. Figure 4 shows the processing scheme which will be described in more detail in the following. The OI scheme is used to get an objective estimate of val-

ues at unobserved locations. The basic equation is:

$$\vec{Z}_a = \vec{Z}_b + \mathbf{K}[\vec{Z}_o - H(\vec{Z}_b)], \quad (1)$$

where the vector \vec{Z}_a is the analysis field that represents the merged CS2-SMOS ice thickness retrieval which we aim for. \vec{Z}_b is the background field vector and \vec{Z}_o the vector that contains all observations (SMOS and CS2). As observations we define already gridded thickness estimates, based on weekly averages as shown in Figure 2. We do this to reduce statistical uncertainties and to provide rather equally distributed observations, which improves the performance of the OI. Furthermore, it is reasonable to reduce the number of observations, otherwise computing can become expensive. Moreover, we assume that the observations are static, which is a simplification, because the satellite thickness estimates are temporally dependent due to ice dynamics and ice drift. Therefore, we neglect any temporal correlations. H is an operator that transforms the background field into the observation space. To be more specific, this is realized by an inverse distance interpolation method. We aim to retrieve weekly analysis fields, based on calendar weeks that reach from Monday to Sunday. Melting does not allow to retrieve summer sea-ice thickness estimates neither from CS2 nor SMOS. Hence, the merged product is limited to the period from October to April.

2.1 Data Sources

As input ice thickness data we use the AWI CS2 product (processor version 1.2) (Ricker et al., 2014; Hendricks et al., 2016) and the SMOS sea-ice thickness retrieval from the University of Hamburg (processor version 3.1) (Tian-Kunze et al., 2014; Kaleschke et al., 2016). As auxiliary data we use ice concentration and ice type provided by the Ocean and Sea Ice Satellite Application Facility (OSI SAF). Table 1 summarizes the different input grids and their spatial resolution.

2.2 The Background Field

The CS2 weekly products leave gaps due to the incomplete orbital coverage (Figure 2a). Therefore, we compute an averaged composite of weekly retrievals, ranging from 2 weeks

Table 1: Properties of input and output data grids, which are used to obtain the merged product.

Product	Source	Frequency	Spatial coverage	Grid/resolution
SMOS Ice Thickness	icdc.zmaw.de/daten	Daily	Entire Arctic	Polarstereo 12.5 km
CS2 Ice Thickness	data.seaiceportal.de	Weekly	Incomplete	EASE2 25 km
Ice Concentration	osisaf.met.no/p/ice/	Daily	Entire Arctic	Polarstereo 10 km
Ice Type	osisaf.met.no/p/ice/	Daily	Entire Arctic	Polarstereo 10 km
Merged Product	data.seaiceportal.de	Weekly	Entire Arctic	EASE2 25 km

behind to two weeks ahead, to get a nearly complete coverage for the Arctic (Figure 5) at a certain target week.

The daily SMOS retrievals are averaged weekly and then re-gridded on an EASE2 25 km grid to be in line with the CS2 retrieval. Here, we only allow SMOS thickness values with a corresponding uncertainty < 1 m, which corresponds to a maximum theoretical thickness of about 1.1 m. Furthermore we expect strong biases for the SMOS ice thickness in thicker MYI regimes. Therefore we apply the OSI SAF ice type product (Eastwood, 2012) and discard any SMOS grid cells that are indicated as MYI. The weekly composites of CS2 and SMOS are shown in Figure 2.

The initial background field is then represented by a weighted average:

$$\bar{Z} = \frac{Z_{cs2}/\sigma_{cs2}^2 + Z_{smos}/\sigma_{smos}^2}{1/\sigma_{cs2}^2 + 1/\sigma_{smos}^2}, \quad (2)$$

Z is the ice thickness and σ the statistical uncertainty of the individual products. Since we use CS2 and SMOS retrievals for the background field beyond the target week and because the SMOS composite contains artifacts of very thin ice (< 10 cm) in coastal regions, we additionally use an ice concentration mask, likewise a weekly mean of daily retrievals from the OSI SAF ice concentration product (Eastwood, 2012) to guarantee the ice coverage during the target week. Here, we use a threshold of 15% and only grid cells which exceeds this value will be considered as ice covered, which corresponds to the ice extent products provided by OSI SAF and the National Snow and Ice Data Center (NSIDC). Gaps in the weighted average, derived from Eq. 2 are interpolated by a nearest neighbor scheme. In order to reduce noise, the

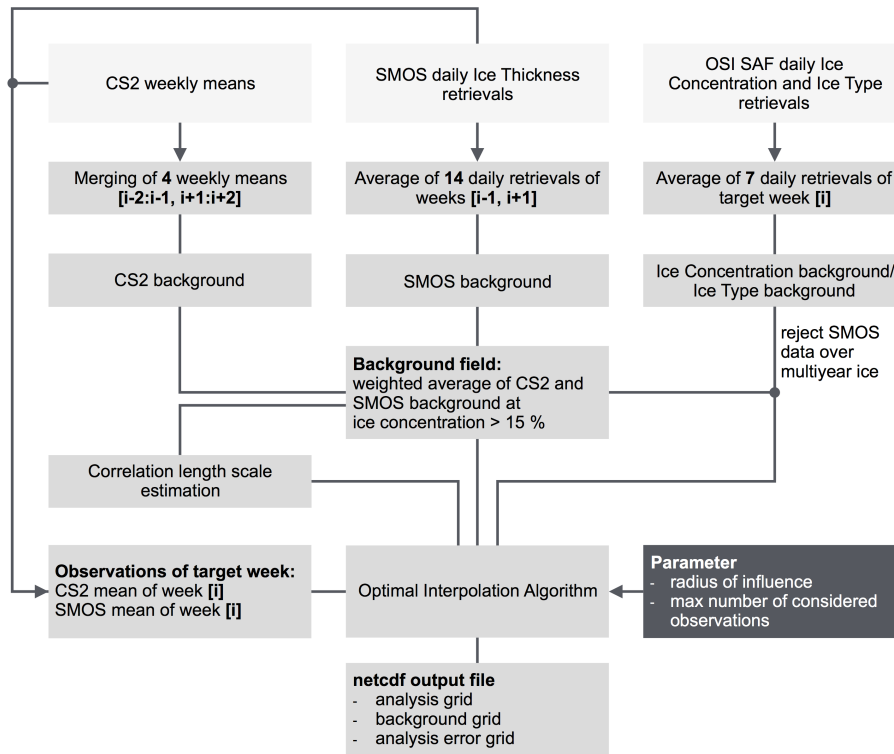


Figure 4: optimal interpolation processing scheme. Week [i] represents the target week. The cycle is repeated for each week.

background field is low-pass filtered before it is used for optimal interpolation (Figure 5b).

2.3 The Optimal Interpolation Algorithm

The weight matrix \mathbf{K} , which is needed to calculate \vec{Z}_a , is retrieved by the background error covariance matrix \mathbf{B} in the observation space multiplied by the inverted total error covariance matrix:

$$\mathbf{K} = \mathbf{B}\mathbf{H}^T(\mathbf{R} + \mathbf{H}\mathbf{B}\mathbf{H}^T)^{-1}, \quad (3)$$

where \mathbf{R} is the error covariance matrix of the observations. In order to reduce computation expense we do several assumptions:

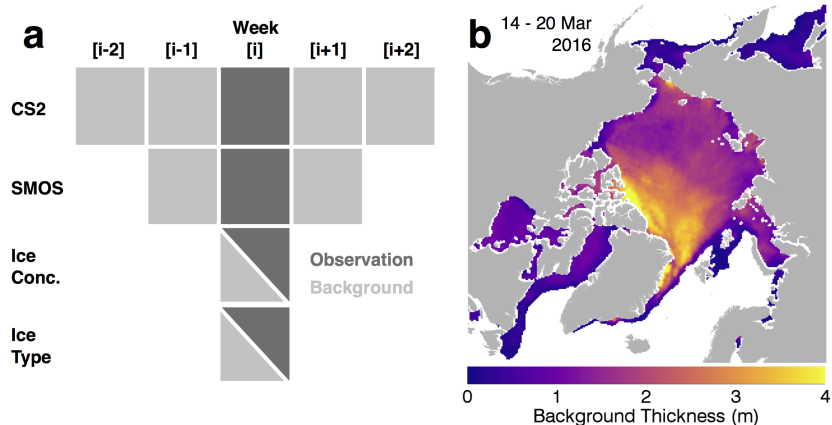


Figure 5: a) The scheme illustrates the usage of weekly input grids for the background field and the observation field. Week [i] represents the target week. b) Interpolated and low-pass filtered background field as it is used for the optimal interpolation.

1. We neglect correlations of observation errors which means that \mathbf{R} is a matrix with non-zero elements only on the diagonal. These variances are represented by the SMOS and CS2 product uncertainties.
2. We assume that the influence of observations that are located far away from the analysis grid point can be neglected. Therefore, instead of computing the entire covariance matrix, we only consider observations within a radius of influence. This radius is set to 250 km to gather just enough observations in regions which large gaps, for example over thick MYI, between two CS2 orbits where valid SMOS observations do not exist.
3. To further reduce computation expense we limit the number of matched observations to 120, meaning that in the case of more matches, only the 120 closest observations are considered.
4. We generally assume that all observations are unbiased, which might be not true in any case (Ricker et al., 2014).

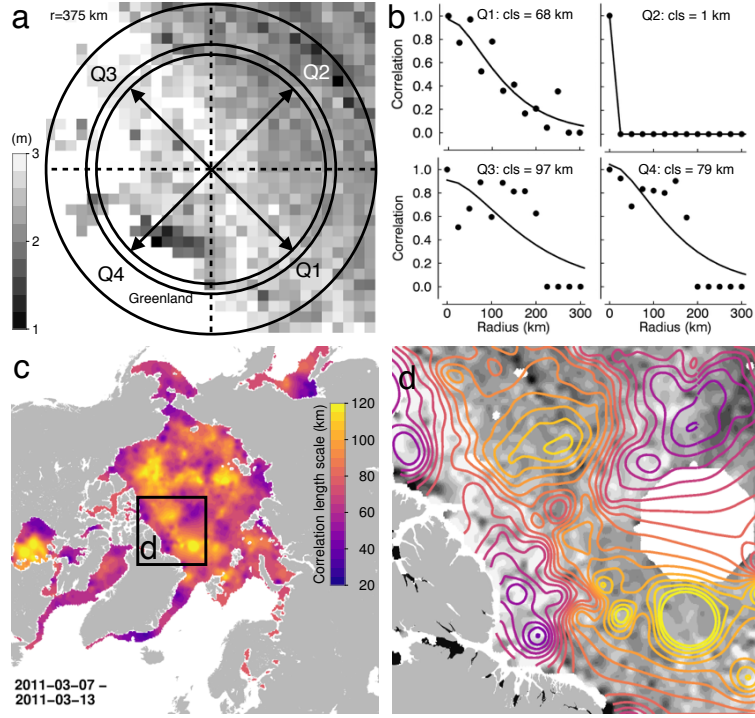


Figure 6: Estimation of the correlation length scale (ξ) for a single grid cell (a): adjacent ice thickness grid cells within a radius of 375 km are binned into annuli of distance and 4 quadrants. (b) Binned thickness estimates are used to calculate the structure function of each quadrant. The ξ is estimated by fitting an exponential function. c) Map of estimated correlation length scales for the 1st week of March 2011. d) The enlarged area shows contoured length scales on top of gray-scaled background thickness with the color scale as in a).

For practical reasons, we apply an iterative computation instead of applying the general matrix formulation in Eq. (1) and Eq. (3). We iteratively calculate each element $z_{a_{m,n}}$ of the analysis field. Vector elements $(bh^T)_i$ and matrix elements $(hbh^T)_{i,j}$ are estimated using a Markov form as a function of the distance to estimate bh^T and hbh^T :

$$\begin{aligned}
 (bh^T)_i &= \left(1 + \frac{d(x_{o_i}, x_{a_{m,n}})}{\xi_{m,n}}\right) \exp\left(\frac{-d(x_{o_i}, x_{a_{m,n}})}{\xi_{m,n}}\right), \\
 (hbh^T)_{i,j} &= \left(1 + \frac{d(x_{o_i}, x_{o_j})}{\xi_{m,n}}\right) \exp\left(\frac{-d(x_{o_i}, x_{o_j})}{\xi_{m,n}}\right),
 \end{aligned} \tag{4}$$

with the Euclidian distance function:

$$d(x, y) = \|x - y\| \quad (5)$$

Here, x_{o_i} and x_{o_j} represent the locations of the matched observations within the radius of influence. $x_{a_{m,n}}$ refers to the location of the analysis grid cell. As a consequence of Eq. (4), the impact of a data point decreases with increasing distance. The estimation of ξ is described in section 2.4.

After computing \mathbf{BH}^T and \mathbf{HBH}^T , yielding \mathbf{K} , we retrieve the second term of Eq. 1, which is called innovation. This iterative procedure is done for every analysis grid point, leading us to the complete analysis field \vec{Z}_a .

2.4 Correlation Length Scale Estimation

The correlation length scale ξ controls how strong the exponential function in Eq. 4 decreases with distance. Since we work on a 25 km grid, we will only consider large scale correlations. Ideally, our correlation length scale estimate is large in the center of a certain ice type regime with similar ice thickness (i.e. first year ice). On the other hand, we expect a low ξ value at locations with a strongly varying thickness gradient. In order to estimate the spatial distribution of ξ , we consider the unfiltered background field \vec{Z}_a . In the following we define a structure function ϵ^2 , which is related to the normalized auto correlation function $R(d, Q)$ as follows (Böhme and Send, 2005):

$$\begin{aligned} \epsilon^2(d, Q) &= \overline{(Z'_0 - Z'_{Q,d})^2} = 2\overline{\sigma_{Z'}^2} - 2\overline{\sigma_{Z'}^2} R(d, Q), \\ R(d, Q) &= 1 - \frac{\epsilon^2(d, Q)}{2\overline{\sigma_{Z'}^2}}. \end{aligned} \quad (6)$$

We define quadrants Q to accommodate the anisotropy of the spatial ice thickness distribution (Figure 6a). $\epsilon^2(d, Q)$ represents the square differences between ice thickness of the grid cell and the ice thickness of the grid cells of binned 25 km distances d in a quadrant Q . $Z'_{Q,d}$ is the unfiltered background thickness, binned according to d and Q . $\overline{\sigma_{Z'}^2}$ are the corresponding mean variances of a certain quadrant. With Eq. 6 we can then obtain the auto correlation function $R(d, Q)$, which is computed up to radius of 750 km (30 bins). In the next step, we fit a Markov function to $R(d, Q)$ and therefore get an estimate for ξ . Figure 6 shows how ξ is derived. Figure 6a reveals the

annuli of distance and the 4 Quadrants. Figure 6b shows the calculated auto correlation function $R(d,Q)$ and the fitted Markov function. Note the strong decrease of $\epsilon^2(d,Q)$ in Q2, which is because Z_0 belongs to a thicker ice regime, while the regime in Q3 is consistently thinner. Therefore $\epsilon^2(d,Q)$ rises, while $\overline{\sigma_{Z'}^2}$ is small. This leads to a strong decrease of $R(d,Q)$ with the distance. $R(d,Q)$ can also become negative if $\epsilon^2(d,Q)/2\overline{\sigma_{Z'}^2}$ gets >1 . In order to enhance the fitting performance, we set $R(d,Q) = 0$ if $R(d,Q) < 0$. Furthermore ξ is set to NaN (not-a-number) if the computation failed. Finally, we take the mean of the ξ values from the 4 quadrants. In order to remove outliers and noise, the derived ξ grid is low-pass filtered with a smoothing radius of 25 km. Invalid grid cells are interpolated by a nearest neighbor scheme afterwards. Figure 6c shows the spatial correlation length scales ξ for 7-13 March 2011. The enlarged area in Figure 6d shows how the ξ decreases in areas with high sea ice thickness gradients.

2.5 The Analysis Error Field

The analysis error covariances are derived by:

$$\sigma_{Z_a}^2 = (\mathbf{I} - \mathbf{KH})\mathbf{B}, \quad (7)$$

Since we consider variances exclusively, we only calculate the diagonal elements of the error covariance matrix. Figure 7 shows the merged product and furthermore the innovation field and the analysis error, which is the root of the error variance. The analysis thickness uncertainty is a relative quantity ranging between 0 and 1, scaled with observation variances. It increases where the weekly CS2 retrieval leaves gaps and where valid SMOS observations are not available, for example at the North Pole or over MYI. In this case the analysis heavily depends on the background field, and therefore the error increases.

3 Dynamic Range of the merged Product

Figure 8 shows ice thickness distributions of monthly means of CS2 and SMOS ice thickness retrievals and the weekly merged product during the freezing season 2015/16. It illustrates the different thickness domains of CS2 and SMOS. The CS2 retrieval lacks

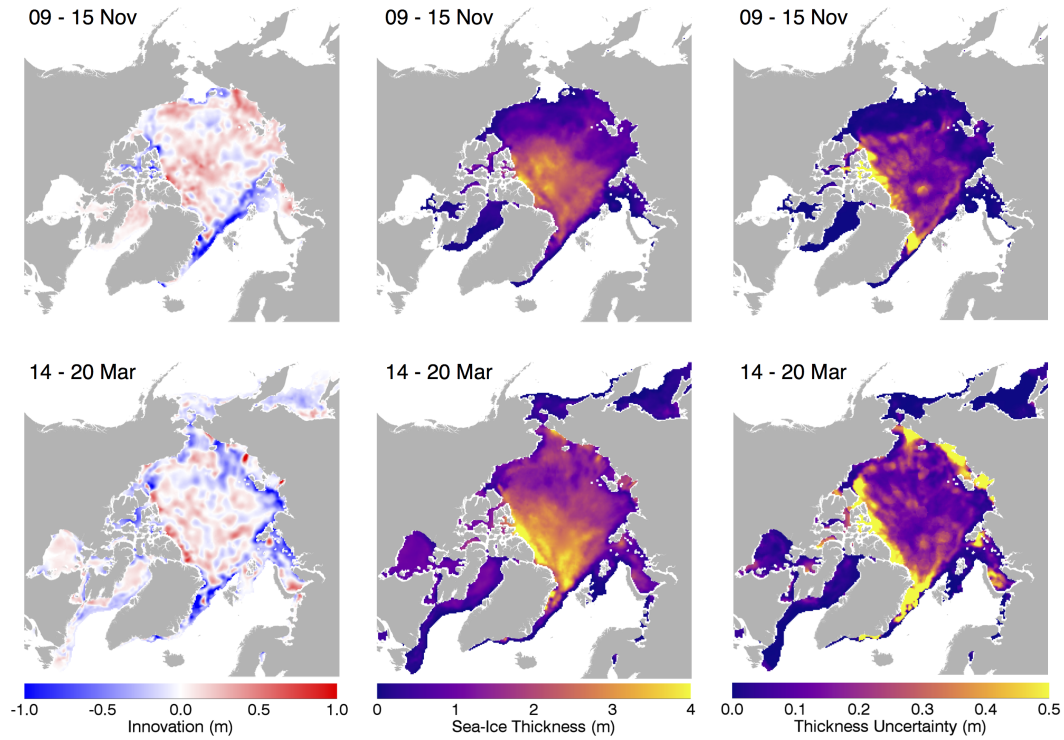


Figure 7: Output grids from the optimal interpolation processing for weeks in November 2015 and March 2016: The innovation (left column) is the difference between background and the merged product ice thickness (center column). The sea-ice thickness uncertainty of the optimal interpolation product is derived from the relative analysis error, scaled with the observation variances (right column).

sensitivity for thin ice (< 0.8 m). This gap can be closed by the SMOS retrieval. Due to the lack of sensitivity over thick ice and the maximum uncertainty filter, the frequency drops steeply at about 1 m. The merged product shows its capability to combine both the CS2 and the SMOS ice thickness domains.

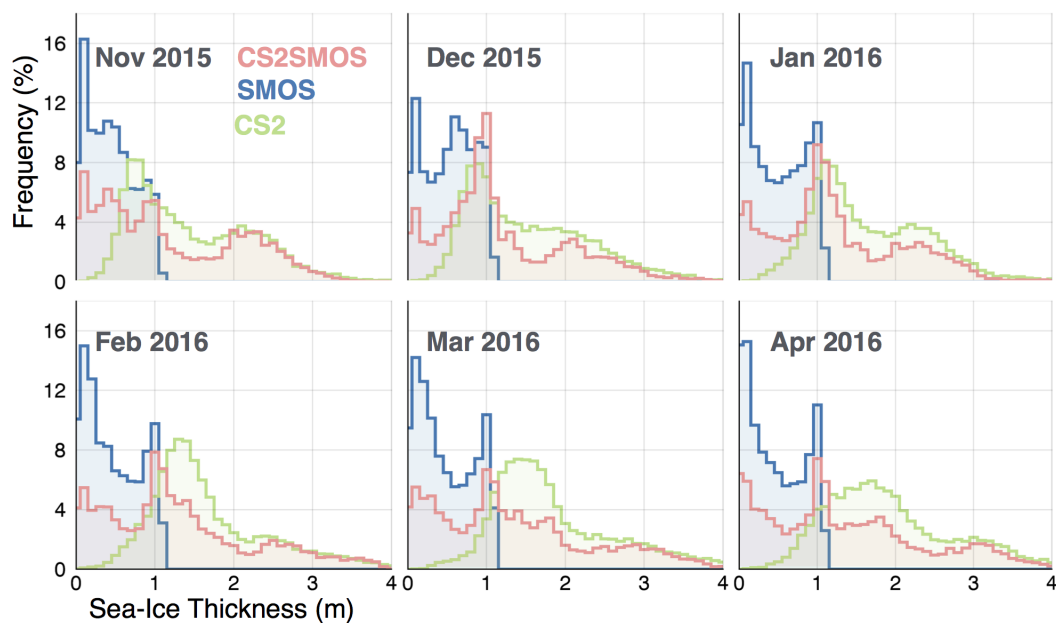


Figure 8: Sea-ice thickness distributions corresponding to Figure 2 during the winter season 2015/16. The merged product is represented by one week within each month, while the CryoSat-2 and SMOS retrievals are monthly means.

4 Data Description

The weekly analysis grids are given in standardized binary data format (Network common data form: NetCDF v4). The variables are given as grid arrays, see therefore Table 2. All grids are projected onto the 25 km EASE2 Grid, which is based on a polar aspect spherical Lambert azimuthal equal-area projection (Brodzik et al., 2012) (Figure 9).

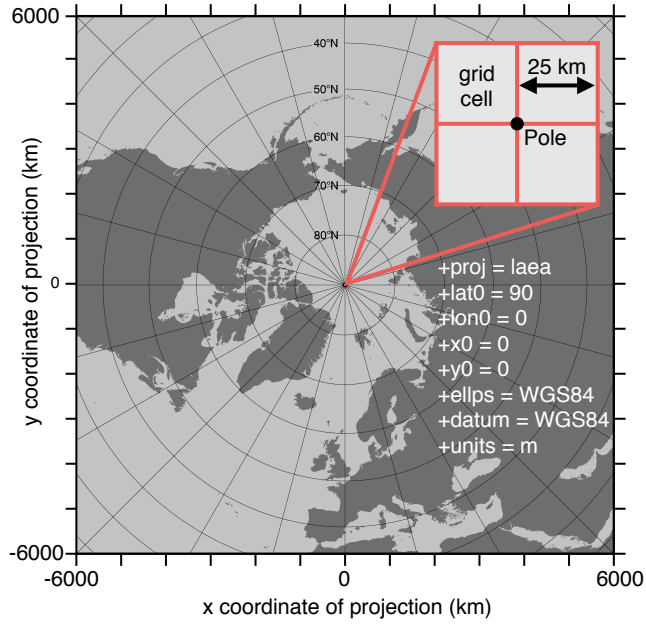


Figure 9: Specifications of the EASE2 25 km grid, which is used for the merged product.

Table 2: Netcdf file content and description of variables.

Variable	Description	Unit	Type	Dimension
time_bnds	Start and stop time	days	double	2
xc	EASE2 grid x coordinates	km	double	720
yc	EASE2 grid y coordinates	km	double	720
longitude	Longitude	deg east	double	720,720
latitude	Latitude	deg north	double	720,720
analysis_thickness	Analysis sea-ice thickness	m	float	720,720
analysis_thickness_unc	Uncertainty of the analysis thickness	m	float	720,720
weighted_mean	Weighted mean of CS2 and SMOS	m	float	720,720
background_thickness	Sea-ice thickness background field	m	float	720,720
corr_scale	Correlation length scale	m	float	720,720
cs2_thickness	Weekly averaged CS2 thickness	m	float	720,720
smos_thickness	Weekly averaged SMOS thickness	m	float	720,720
innovation	Difference background/analysis field	m	float	720,720
ice_concentration	Sea-ice concentration (from OSI SAF)	%	float	720,720
ice_type	Sea-ice type (from OSI SAF)	binary	float	720,720

Acknowledgements

This work has been conducted in the framework of the European Space Agency project SMOS+ Sea Ice (contracts 4000101476/10/NL/CT and 4000112022/14/I-AM). Lars Kaleschke was responsible for the coordination and design of the SMOS+ Sea Ice project. Many thanks go to Matthias Drusch and the entire SMOS+ Sea Ice Team. Moreover, this study is associated with the Deutsche Forschungsgemeinschaft (DFG EXC177) and the German Federal Ministry of Economics and Technology (Grant 50EE1008). CryoSat-2/SMOS data from 2010-2016 are provided by <http://www.meereisportal.de> (Grant REKLIM-2013-04).

References

- Boehme, L., Meredith, M. P., Thorpe, S. E., Biuw, M., and Fedak, M.: Antarctic Circumpolar Current frontal system in the South Atlantic: Monitoring using merged Argo and animal-borne sensor data, *Journal of Geophysical Research: Oceans*, 113, doi: 10.1029/2007JC004647, URL <http://dx.doi.org/10.1029/2007JC004647>, c09012, 2008.
- Böhme, L. and Send, U.: Objective analyses of hydrographic data for referencing profiling float salinities in highly variable environments, *Deep Sea Research Part II: Topical Studies in Oceanography*, 52, 651–664, 2005.
- Brodzik, M. J., Billingsley, B., Haran, T., Raup, B., and Savoie, M. H.: EASE-Grid 2.0: Incremental but Significant Improvements for Earth-Gridded Data Sets, *ISPRS International Journal of Geo-Information*, 1, 32–45, doi:10.3390/ijgi1010032, URL <http://www.mdpi.com/2220-9964/1/1/32>, 2012.
- Eastwood, S.: OSI SAF Sea Ice Product Manual, v3.8 edn., URL <http://osisaf.met.no>, 2012.
- Hendricks, S., Ricker, R., and Helm, V.: User Guide - AWI CryoSat-2 Sea Ice Thickness Data Product (v1.2), 2016.
- Kaleschke, L., Tian-Kunze, X., Maaß, N., Mäkynen, M., and Drusch, M.: Sea ice thickness retrieval from SMOS brightness temperatures during the Arctic freeze-up period, *Geophysical Research Letters*, 39, 2012.

- Kaleschke, L., Tian-Kunze, X., Maas, N., Ricker, R., Hendricks, S., and Drusch, M.: Improved retrieval of sea ice thickness from SMOS and CryoSat-2, in: Geoscience and Remote Sensing Symposium (IGARSS), 2015 IEEE International, pp. 5232–5235, IEEE, 2015.
- Kaleschke, L., Tian-Kunze, X., Maaß, N., Beitsch, A., Wernecke, A., Miernecki, M., Müller, G., Fock, B. H., Gierisch, A. M., Schlünzen, K. H., Pohlmann, T., Dobrynin, M., Hendricks, S., Asseng, J., Gerdes, R., Jochmann, P., Reimer, N., Holfort, J., Melsheimer, C., Heygster, G., Spreen, G., Gerland, S., King, J., Skou, N., Søbjerg, S. S., Haas, C., Richter, F., and Casal, T.: {SMOS} sea ice product: Operational application and validation in the Barents Sea marginal ice zone, *Remote Sensing of Environment*, 180, 264 – 273, doi:<http://dx.doi.org/10.1016/j.rse.2016.03.009>, URL <http://www.sciencedirect.com/science/article/pii/S003442571630102X>, special Issue: ESA's Soil Moisture and Ocean Salinity Mission - Achievements and Applications, 2016.
- McIntosh, P. C.: Oceanographic data interpolation: Objective analysis and splines, *Journal of Geophysical Research: Oceans* (1978–2012), 95, 13 529–13 541, 1990.
- Ricker, R., Hendricks, S., Helm, V., Skourup, H., and Davidson, M.: Sensitivity of CryoSat-2 Arctic sea-ice freeboard and thickness on radar-waveform interpretation, *The Cryosphere*, 8, 1607–1622, doi:10.5194/tc-8-1607-2014, URL <http://www.the-cryosphere.net/8/1607/2014/>, 2014.
- Ricker, R., Hendricks, S., Perovich, D. K., Helm, V., and Gerdes, R.: Impact of snow accumulation on CryoSat-2 range retrievals over Arctic sea ice: An observational approach with buoy data, *Geophysical Research Letters*, 42, 4447–4455, doi:10.1002/2015GL064081, URL <http://dx.doi.org/10.1002/2015GL064081>, 2015GL064081, 2015.
- Tian-Kunze, X., Kaleschke, L., Maaß, N., Mäkynen, M., Serra, N., Drusch, M., and Krumpen, T.: SMOS-derived thin sea ice thickness: algorithm baseline, product specifications and initial verification, *The Cryosphere*, 8, 997–1018, doi:10.5194/tc-8-997-2014, URL <http://www.the-cryosphere.net/8/997/2014/>, 2014.
- Wingham, D., Francis, C., Baker, S., Bouzinac, C., Brockley, D., Cullen, R., de Chateau-Thierry, P., Laxon, S., Mallow, U., Mavrocordatos, C., Phalippou, L., Ratier, G., Rey, L., Rostan, F., Viau, P., and Wallis, D.: CryoSat: A mission to determine the fluctuations

in Earth's land and marine ice fields, *Advances in Space Research*, 37, 841 – 871,
doi:10.1016/j.asr.2005.07.027, 2006.